Soft ionization of thermally evaporated hypergolic ionic liquid aerosols

Christine J. Koh[†], Chen-Lin Liu[‡,⊥], Christopher W. Harmon[‡], Daniel Strasser[†,#], Amir Golan[‡], Oleg Kostko[‡], Steven D. Chambreau[§], Ghanshyam L.Vaghjiani[||], and Stephen R. Leone[†,‡,]*

Departments of Chemistry and Physics, University of California, Berkeley, California 94720, Chemical Sciences Division, Lawrence Berkeley National Laboratory, Berkeley, California 94720, ERC, Incorporated and Air Force Research Laboratory, Edwards Air Force Base, California 93524

---

[*] To whom correspondence should be addressed. Email: srl@berkeley.edu

† University of California.

‡ Lawrence Berkeley National Laboratory.

§ ERC, Incorporated, Edwards Air Force Base.

|| Air Force Research Laboratory, Edwards Air Force Base.

⊥ Present affiliation: National Synchrotron Radiation Research Center (NSRRC), Hsinchu 30076, Taiwan.

Present affiliation: Institute of Chemistry, Hebrew University, Jerusalem 91904, Israel.

srl@berkeley.edu

Received: March 16, 2012; Revised Manuscript Received: March 16, 2012

TITLE RUNNING HEAD: Soft ionization of evaporated IL aerosols

Isolated ion pairs of a conventional ionic liquid, 1-Ethyl-3-Methyl-Imidazolium Bis(trifluoromethylsulfonyl)imide ($[Emim^+][Tf_2N^-]$), and a reactive hypergolic ionic liquid, 1-Butyl-3-Methyl-Imidazolium Dicyanamide ($[Bmim^+][Dca^-]$), are generated by vaporizing ionic liquid submicron aerosol particles for the first time; the vaporized species are investigated by dissociative ionization with tunable vacuum ultraviolet (VUV) light, exhibiting clear intact cations, $Emim^+$ and $Bmim^+$, presumably originating from intact ion pairs. Mass spectra of ion pair vapor from an effusive source of the hypergolic ionic liquid show substantial reactive decomposition due to the internal energy of the molecules emanating from the source. Photoionization efficiency curves in the near threshold ionization region of isolated ion pairs of $[Emim^+][Tf_2N^-]$ ionic liquid vapor are compared for an aerosol source and an effusive source, revealing changes in the appearance energy due to the amount of internal energy in the ion pairs. The aerosol source has a shift to higher threshold energy (~0.3 eV), attributed to reduced internal energy of the isolated ion pairs. The method of ionic liquid submicron aerosol particle vaporization, for reactive ionic liquids such as hypergolic species, is a convenient, thermally "cooler" source of isolated intact ion pairs in the gas phase compared to effusive sources.

Keywords: ionic liquid, aerosol, ion pair, gas phase, photoionization efficiency, synchrotron

Introduction

Ionic liquids (ILs) are ambient temperature molten salts[1] with fascinating properties, including extremely low volatility, tunable chemical properties, and distinctive reactivity.[2-11] The unique properties of ILs are a direct result of the interactions between the ions[12,13] and this led to an explosion of interest to utilize ILs for broad applications such as catalysts,[14] batteries,[8,9,15] and hypergolic fuels.[16-19] Some energetic ionic liquids, the dicyanamide,[16] nitrocyanamide,[19] and azide systems,[17] have shown promising potential for propellant applications,[18] as substitutes for conventional energetic compounds, monomethyl hydrazine/nitrogen tetroxide (MMH/NTO), with several advantages including thermal stability, environmental friendliness, and low volatility. For the task-specific use of ILs, they can be designed accordingly by varying the choices of the cation-anion combinations. Physicochemical properties of ILs change dramatically based on the constituents, and Plechkova and Seddon[20] estimate that possible ion pairings can be as many as 10^{18}. This vast number of possible combinations makes it almost impossible to test all available ILs for specific applications. It is therefore valuable to understand in greater depth the fundamental properties of the isolated ion-pairs and to extrapolate and predict the features of ILs.

Recent studies[21-33] show that isolated ion-pairs can be prepared in the gas phase by thermal vaporization of ILs despite their extremely low vapor pressure. Earle and collaborators[34] reported in 2006 that intact cations (C^+) and anions (A^-) associated in the vapor are produced by vaporization, and this result initiated multiple studies that investigate the vaporization mechanism and the nature of IL vapor.[23-32] Various experimental methods, such as soft ionization mass spectrometry,[26,29] line-of-sight mass spectrometry,[21,24] UV spectroscopy[23] and cryogenic neon matrix-isolation FTIR spectroscopy,[27] provide direct evidence of the existence of

vaporized ion pairs in the form of cation-anion 1:1 pairs. Ionization of these vaporized ion pairs by photons or electrons often produces intact cations (C^+) as a result of dissociative ionization (eq 1).

$$C^+A^- \rightarrow C^+ + A + e^- \quad (1)$$

Intact cations are observed whether the origin of the ion pair vapor is a bulk sample or a thin film heated for the vaporization. However, highly reactive ionic liquids show dissociative ionization as well as decomposition, and it becomes difficult to identify the intact cation signal and to distinguish thermal decomposition from fragmentation of ion pairs upon ionization. This makes it nearly impossible to study reaction mechanisms and kinetics of hypergolic ionic liquids because of the difficulty of detecting small changes in their complicated mass spectra.

Typically ions with high internal energies fragment extensively producing a mass spectrum that contains a wide variety of abundant fragment ions.[35] The internal energy content of the molecular ion (M^+) is from two sources: the thermal energy from evaporation and the energy imparted by the ionization process. Molecular ions (M^+) of labile molecules can only be detected if the internal energy of the molecular ion is kept very low, by obtaining mass spectra with low photon energies and low temperatures. Aerosol particle generation[36-41] has previously been demonstrated as a new way to introduce fragile biomolecules into the gas phase with nearly fragmentation-free mass spectra by minimizing their internal energy imparted into the molecular ion in gas phase. We apply this new method to hypergolic IL studies, to produce isolated ion pairs in the gas phase from IL aerosol particles followed by thermal vaporization, and monitor the ion pair vapor by soft ionization using tunable vacuum ultraviolet (VUV) photoionization mass spectrometry. This report focuses on comparing the degree of fragmentation depending on the isolated ion pair vapor source of a hypergolic ionic liquid, 1-Butyl-3-Methyl-Imidazolium

Dicyanamide ([Bmim$^+$][Dca$^-$]), shown in Figure 1(b), and on finely controlling the internal energy imparted by thermal vaporization and photoionization. For a better understanding of the internal energy extent originating from different ion pair vapor sources, effusive and aerosol, the appearance energy shifts of 1-Ethyl-3-Methyl-Imidazolium Bis(trifluoromethylsulfonyl)imide ([Emim$^+$][Tf_2N^-]) ionic liquid vapor are measured by photoionization efficiency (PIE) curves at the same vaporization temperatures, clearly showing the effect that the vapor source has on the ion pairs.

Experimental Apparatus

Isolated ion pairs of ionic liquids are generated in the gas phase by thermal vaporization of IL aerosol particles and are monitored using soft ionization detection with tunable vacuum ultraviolet (VUV) photoionization mass spectrometry. Those ion pairs that are generated by aerosol particles are compared to those generated by a conventional effusive beam.[26,28,29] The aerosol experimental apparatus at the Chemical Dynamics Beamline 9.0.2.1 of the Advanced Light Source in Berkeley, California, previously described in detail,[35] includes a particle generation system, a particle size analyzer, and an aerosol mass spectrometer (AMS).

Ionic liquid aerosols are generated by a constant output atomizer (TSI model no. 3076) from 0.5 g/L in water solutions of ionic liquid, [Emim$^+$][Tf_2N^-] (Sigma, ≥97% purity) or [Bmim$^+$][Dca$^-$]) (Aldrich, ≥97% purity), structures shown in Figure 1. Generated liquid droplets are then entrained in a nitrogen carrier gas at 10 psi and are dried by passing through a room-temperature diffusion dryer with a small chance of water still remaining in the particles. The aerosol particle size distribution and number density are measured with a commercial differential mobility analyzer (DMA; TSI model 3081) coupled to a condensation particle counter (CPC; TSI

model 3772). Aerosol particles of [$Emim^+$][Tf_2N^-] produced in this way have a median diameter of 187 ± 3 nm, as shown in Figure 2(a), and a total concentration of 1.4×10^5 particles/cm^3, where similarly produced aerosol particles of [$Bmim^+$][Dca^-] have a median diameter of 184 ± 3 nm (Figure 2(b)) and a total concentration of 2.0×10^5 particles/cm^3. To generate isolated ion pairs in the gas phase, the dry aerosol particles, focused through the aerodynamic lens with a particle flux of about 3×10^7 particles/s entering the interaction region,[38] are thermally vaporized by a heated copper block typically held at a temperature between 423 K and 493 K. In all cases, ionic liquids, [$Emim^+$][Tf_2N^-] and [$Bmim^+$][Dca^-], were kept well under their thermal decomposition temperatures (T_d), which are 675 K[1] and 573 K,[42] respectively. The vapor from aerosol particles provides isolated ion pairs and the mass spectra are followed by VUV photoionization to produce positive ions by single photon ionization. The time-of-flight (TOF) mass spectra and ion yields are measured with a pulsed TOF mass spectrometer and recorded as a function of the heater temperature and the photon energy of the tunable VUV source, between 7.5 and 11 eV in 75 meV steps, for each ionic liquid.

In the other sets of experiments, isolated ion pairs are prepared as an effusive beam, which is a typical pyrolysis source using an aluminum oven body with a glass interior heated by resistive heater cartridges. The glass interior prevents IL sample vapor from colliding with the aluminum wall, and there is no evidence for decomposition. IL sample is heated to 350 K overnight prior to experiments in order to remove contaminants. IL vapor is emitted through an opening in the oven as an effusive beam by heating the 0.5 ml size reservoir of a glass vial located in the aluminum oven.[26,28,29] The effusive beam is skimmed by an ~1 mm skimmer before the beam is ionized by the VUV light. Similar to the experiments for ion pairs from the aerosol particles, TOF mass spectra and ion yields of the positive ions produced by photoionization of the effusive beam are

recorded as a function of photon energy, tunable between 7.5 eV and 11 eV in 50 meV steps. All of the measurements, mass spectra, PIE scans, and heater block temperature scans, for two different sources (aerosol, and effusive source) were measured at least five, two, and three times, respectively. Temperature scans of the aerosol source were not only repeated but also measured while both heating and cooling the heater block in order to ensure that there is not thermal decomposition occurring during heating. Collected PIE curves were rebinned into 0.2 eV step data sets for comparison of the two sources, effusive beam and aerosol source beam.

Results and Discussion

Isolated ion pairs of ionic liquids are prepared in the gas phase by thermally vaporizing from submicron aerosol particles with median diameter around 180 nm; the particle size distribution is shown in Figure 2. These ion pairs in the effusive and aerosol source beam are monitored by near threshold photoionization with mass resolutions of 480 and 1061 at 96 amu/q, respectively. Both ionic liquids studied here, $[Emim^+][Tf_2N^-]$ and $[Bmim^+][Dca^-]$, show the intact cation signal, which is an indication of isolated ion pairs. The intact cation signals, $Emim^+$ (111 amu/q), from $[Emim^+][Tf_2N^-]$ in the effusive beam (top) and aerosol source beam (bottom) are shown in Figure 3(a) and are highlighted in grey color. The intact cation signal dominates in both mass spectra, whereas the aerosol source beam shows small hydrogen loss from the intact cation as well. The hydrogen loss from the intact cation that is ca. 0.5% signal of intact cation can originate by proton transfer from the ionic liquid to the solvent since the submicron aerosol particles have a trace of water remaining in the particles. This hydrogen loss from the ionic liquid during aerosol generation is being studied further. However it is noteworthy that isolated ion pairs from the aerosol source of $[Emim^+][Tf_2N^-]$ are successfully prepared. Whether those

pairs have some associated water molecules may be revealed by tunable photon energy ionization studies. In the case of DNA bases, the addition of water molecules in cluster studies reveals both masses containing water and shifts in the ionization energies.[43]

To further explore the isolated ion pair and its internal energy depending on the type of vapor source, photoionization efficiency (PIE) curves of the intact cation $Emim^+$ for the ionic liquid $[Emim^+][Tf_2N^-]$ were measured, as shown in Figure 3. The two different sources are the aerosol and effusive source. Unfortunately, the changes in the appearance energy of the intact cation from the hypergolic ionic liquid, $[Bmim^+][Dca^-]$, could not be directly measured because of the limited signal of the intact cation for the effusive beam, as shown in the mass spectra of Figure 4. The shift in appearance energy in the near-threshold ionization region for $[Emim^+][Tf_2N^-]$ was therefore explored at 493 K for the two sources, as a measure of the internal energy. The photoionization efficiency curve of the intact cation, $Emim^+$, produced from the aerosol source beam is shown in Figure 3(b). Raw PIE curves (○) of $Emim^+$ produced from vaporization of aerosol particles show an additional low energy component due to a minor contribution from slowly vaporizing residual ionic liquid on the heater block. This contribution from the residual vapor (●) to the PIE curve is measured by turning off the aerosol source, keeping the heater at the same temperature, and scanning the photon energy either increasing or decreasing, in order to make sure there is no artifact coming from sample flux changes while scanning. The pure PIE curve of the immediately vaporized ion pair, shown in Figure 3(b) top (▲), is found by subtracting the normalized residual signal from the total raw PIE curve.

This subtracted signal (▲) that is the PIE curve of the intact cation from dissociative ionization of ion pairs vaporized directly from the aerosol source beam is plotted together with the other PIE curve measured for the effusive beam (○) for comparison in Figure 3(c). Data from

the two sources is rebinned into photon energy steps of 0.2 eV to compare consistent resolution of data sets. Near threshold the PIE curves are fitted similar to previous studies,[29] but they are not convoluted with a Gaussian which was previously used based on the assumption that the source temperature was all the same. The PIE curves are fitted with the functional form $0.5 \cdot \alpha(E-E_0)^2$ with two fit parameters, normalization factor α and the ionization threshold E_0, in order to find the changes in the ionization threshold that is due to the source temperature change. The normalization factor α, which is a fit parameter, takes into account of the molecular density difference of two sources and the PIE curves are fitted in a wide range of photon energy up to 10.8 eV. The solid lines in Figure 3(c) are the fitted threshold functions, corresponding to threshold ionization energies of 8.61 ± 0.12 and 8.93 ± 0.13 eV for the effusive beam and aerosol source beam, respectively. For all experiments, the vaporization temperature was kept at 493 ± 2 K, and thus the observed shifts are not expected to be due to different temperatures of the sources. As expected from previous studies,[38,44] the appearance energy increases from the effusive beam to aerosol source beam. The aerosol source beam shows a +0.3 eV shift toward higher appearance energy compared to the effusive beam. This increased appearance energy of the aerosol source suggests that the aerosol source beam produces ion pair vapor with less internal energy than the effusive beam does. Evaporation of the IL aerosol particles may produce some of the cooling by molecules vaporizing from an impact at the heater block that leads to less internal energy.

The hypergolic ionic liquid is also studied using the aerosol source to produce isolated ion pairs that are internally cooler than those generated by the effusive source. Mass spectra obtained for the hypergolic ionic liquid, $[Bmim^+][Dca^-]$, vaporized at 473 K from both the aerosol and effusive sources are shown in Figure 4. The overall mass spectra of the hypergolic IL vapors

prepared from the effusive and aerosol sources show dramatic differences regardless of the photon energy, (a) 8.5 eV or (b) 9.4 eV, used for ionization. Prominent peaks in the mass spectra of the aerosol source beam are 139 amu, the intact cation, and 137 amu, a fragment of the intact cation in which two hydrogens are lost or a fragment resulting from multiple proton transfers to the solvent as in the $[Emim^+][Tf_2N^-]$ case. On the other hand, mass spectra of the effusive beam do not show any of those intact cation signals, but instead there are evident peaks at 178 and 124 amu. A molecular structure shown in Figure 4 above the 178 amu peak is the strongest candidate for this possible ion species, which is a structurally reorganized fragment of the ion pair from which two hydrogens on the cation have been displaced by the anion fragment, -NCN. The 124 amu peak is assigned either to the cation fragment with the loss of a methyl group or to a decomposition product of 1-Butyl-Imidazolium. Details of the fragments, whether they are from thermal decomposition or dissociative ionization of the effusive beam of the hypergolic ionic liquid, $[Bmim^+][Dca^-]$, are under further investigation. Despite the fact that the photodissociation mechanism and vaporization of the $[Bmim^+][Dca^-]$ ion pair from the effusive beam is not yet established, it is important to note that the photoionization masses change drastically with the source and there is much more extensive fragmentation and formation of new products in the effusive source.

The intact cation, $Bmim^+$ (139 amu), that is observed in the mass spectra of the aerosol source beam is most likely produced by dissociative photoionization (eq 1). This is typical evidence[24,26,29] for the production of an isolated ion pair in the gas phase upon vaporization of $[Bmim^+][Dca^-]$ ionic liquid aerosol particles. There is no indication of ionic liquid clusters with water or extensive thermal decomposition (data not shown) from the aerosol source beam as long as the impact heater temperature is kept lower than would be needed to produce cluster

formation or thermal decomposition (T_d, 573 K[42]). Furthermore no parent ionic liquid mass is observed, similar to previous studies.[24,26,29] The dominant peak other than the intact cation, the loss of two hydrogens from the cation fragment (137 amu), and other small features of 178 and 124 amu mass peaks, which are mainly observed in the effusive beam, suggest that there is enough energy in the aerosol heater zone for the ion pair to dissociatively ionize to other ion species or to decompose into these fragments. The results show that the ion pairs generated from the aerosol source acquire some internal energy that eventually leads to a small amount of dissociative photoionization or decomposition resulting in fragments other than the intact cation upon vaporization or ionization.

In addition to the intact cation ($Bmim^+$, 139 amu) signal, it is also possible to observe the corresponding ^{13}C isotope peak at 140 amu in the mass spectra of the aerosol source beam. The relative yields of the ^{13}C isotope peak, 8.4 ± 0.4% measured at a photon energy of 8.5 eV, and 8.9 ± 0.3% measured at photon energy of 9.4 eV, are in good agreement with the natural isotope abundance, 8.8%, for $Bmim^+$ (139 amu) with eight carbon atoms. The ^{13}C isotope peak of the 137 amu ($[Bmim^+]$–2H) at 138 amu cannot be measured due to the overlapping signal of another 138 amu fragment ($[Bmim^+]$–H). However, if we assume the natural isotope abundance of 8.8% for the unknown $[Bmim^+]$–2H fragment (137 amu) and $[Bmim^+]$–H fragment (138 amu) signal, we can estimate the ratio of fragments to intact cation, $[Bmim^+]$–2H / $[Bmim^+]$–H / $[Bmim^+]$, to be 1.3/0.4/1.0 at 8.5 eV and 1.2/0.2/1.0 at 9.4 eV.

The general difference in the mass spectra of the aerosol source beam and the effusive beam is that the major photofragments from the effusive beam are the minor ones in the mass spectra of the aerosol source beam. Since those minor photofragments of the aerosol source beam, 178, 138, and 124 amu, are due to the excess energy imparted to the isolated ion pair, it shows that the

aerosol beam has isolated ion pairs with considerably less internal energy resulting in much less extensive dissociative ionization and reaction. Ion pairs vaporized from the effusive source have a high probability to gain more energy and possibly react via intermolecular collisions and multiple high temperature wall collisions, resulting in a considerable internal energy, whereas aerosol particles vaporized by an impact at the heater block are both energized and further cooled by evaporation, resulting in an ion pair vapor that has less decomposition or reaction and a lower temperature. This means that the isolated ion pair vapor prepared from aerosol particles has less internal energy imparted upon thermal vaporization compared to those from the effusive beam, which is in good agreement with previous studies,[38] where reduced thermal internal energy content is reported for biomolecules in gas phase produced by aerosol particle vaporization. Therefore, to explore the unique reaction dynamics of hypergolic ionic liquids, aerosol particle vaporization is a suitable way to introduce intact ion pairs into the gas phase to decrease the internal energy, essentially by having only one impact on the heater block to energize and evaporate the molecules into the gas phase.

Another difference in the mass spectra of the aerosol source beam and the effusive beam is that the signal-to-noise of the aerosol source beam measurement (S/N, ca. 800) is better than the effusive beam measurement (S/N, ca. 7). Data for the aerosol source beam is collected for 2,000,000 pulses while the data for the effusive beam is collected for 500,000 pulses, which is 4 times less integration time than the aerosol source beam. If we assume that the signal-to-noise will increase by the square root of the integration time, the mass spectra of the effusive beam will have a signal-to-noise of ca. 14 better at the same integration time as the aerosol source beam measurement. Thus the signal-to-noise in the mass spectra of the aerosol source beam is an order of magnitude greater with the effusive beam after taking into account the integration time

difference. Better signal-to-noise in the mass spectra of the aerosol source beam is probably due to the closer distance of the vaporization source from the ionization region. This shows that the aerosol particle vaporization has the advantage in not only producing molecules with less internal energy, but also in having superior signal-to-noise in TOF measurements.

The influence of the internal energy on photofragmentation of $[Bmim^+][Dca^-]$ ion pairs prepared by the aerosol method is investigated in more detail by monitoring the molecule to fragment ratio as a function of both (a) temperature and (b) photon energy, as shown in Figure 5. The molecule (M) to fragment (F) ratio is determined by the intensity ratio of the intact cation (139 amu), which represents the molecular ion, and the cation fragment with the loss of two hydrogens (137 amu). The M/F ratios decrease with temperature and photon energy as the amount of internal energy imparted into the isolated ion pair increases, thus leading to more dissociative photoionization. At a fixed photon energy, 8.5 eV, the M/F ratio exponentially decreases with temperature over the 50 K range studied and is consistent with the previous effect[38] observed for biomolecules. The exponential decay behavior was suggested[38] to be due to an "Arrenhius-like" phenomenological activation energy, which leads to efficient dissociative photoionization when excess energy is imparted by photoionization into the thermally activated ion pair. The M/F ratio is also observed to decrease as a function of photon energy at a fixed temperature of 473 K. As the photon energy is increased to ionize the neutral ion pair, the amount of internal energy deposited increases and results in greater fragmentation. The intact cation signal used to monitor the isolated ion pairs decreases relative to the fragment signal regardless of the fragment chosen (124, 137, 138, 178 amu, data not shown) as a function of temperature and photon energy. As expected, the highest M/F ratio is observed at the lowest vaporization temperature around 423 K and at the lowest photon energy used for ionization near

threshold (8.0 eV). The results show that the internal energy of ion pairs can be reduced by using near threshold ionization and lower vaporization temperature for nearly "fragmentation-free" mass spectra. This decreased fragmentation of isolated ion pairs from the aerosol source beam clearly affords a number of advantages over conventional effusive beams for monitoring reaction dynamics of hypergolic ionic liquids in the future.

Conclusions

Using aerosol particle vaporization as a source, isolated ion pairs of a hypergolic ionic liquid and a relatively stable ionic liquid are generated in the gas phase and these ion pairs are compared to the ones produced via a conventional effusive beam, all of which are monitored with a tunable synchrotron light source in the near threshold ionization region. Vaporizing ionic liquid aerosol particles reduces the amount of internal energy imparted into the isolated ion pair upon thermal vaporization and minimizes reactive processes. This capability not only affords greater insight into the various methods of generating ion pair vapors, but also provides a better way to monitor reaction dynamics of hypergolic ionic liquids in the future, with simpler photofragmentation patterns of the ion pair itself and fewer complications in tracing molecular changes. Given the distinctively strong intensity of the intact cation and superior signal-to-noise with this aerosol experimental setup, which has also been shown to be capable of studying reaction dynamics,[45] future studies are planned to utilize and apply this technique to further understand hypergolic IL reactivity.

Acknowledgments

The authors gratefully acknowledge funding from the U.S. Air Force Office of Scientific Research for supporting CK, DS and SL (Grant No. FA9550-10-1-0163), and for SC and GV (Grant No. FA9300-06-C-0023). This work at the ALS was supported by the Director, Office of Energy Research, Office of Basic Energy Sciences, Chemical Sciences Division of the U.S. Department of Energy under Contract No. DE-AC02-05CH11231 (CL, CH, AG, OK, KW, MA, and SL). The authors thank Dr. Musahid Ahmed and Dr. Kevin Wilson of the Chemical Dynamics Beamline for help in the measurements.

References

(1) Wasserscheid, P.; W., T. *Ionic liquids in synthesis*, 2 ed.; Wiley-VCH, Weinheim, 2007.

(2) Blanchard, L. A.; Hancu, D.; Beckman, E. J.; Brennecke, J. F. *Nature* **1999**, *399*, 28-29.

(3) Yoshizawa, M.; Xu, W.; Angell, C. A. *J. Am. Chem. Soc.* **2003**, *125*, 15411-15419.

(4) Wang, P.; Zakeeruddin, S. M.; Comte, P.; Exnar, I.; Gratzel, M. *J. Am. Chem. Soc.* **2003**, *125*, 1166-1167.

(5) Wang, P.; Wenger, B.; Humphry-Baker, R.; Moser, J. E.; Teuscher, J.; Kantlehner, W.; Mezger, J.; Stoyanov, E. V.; Zakeeruddin, S. M.; Gratzel, M. *J. Am. Chem. Soc.* **2005**, *127*, 6850-6856.

(6) Castner, E. W.; Wishart, J. F. *J. Chem. Phys.* **2010**, *132*, 9.

(7) Wilkes, J. S. *Green Chem.* **2002**, *4*, 73-80.

(8) Shin, J. H.; Henderson, W. A.; Passerini, S. *Electrochem. Commun.* **2003**, *5*, 1016-1020.

(9) Hu, Y. S.; Li, H.; Huang, X. J.; Chen, L. Q. *Electrochem. Commun.* **2004**, *6*, 28-32.

(10) de Souza, R. F.; Padilha, J. C.; Goncalves, R. S.; Dupont, J. *Electrochem. Commun.* **2003**, *5*, 728-731.

(11) Susan, M.; Noda, A.; Mitsushima, S.; Watanabe, M. *Chem. Commun. (Cambridge, U. K.)* **2003**, 938-939.

(12) Schroder, C.; Steinhauser, O. *J. Chem. Phys.* **2008**, *128*, 7.

(13) Hunt, P. A.; Gould, I. R.; Kirchner, B. *Aust. J. Chem.* **2007**, *60*, 9-14.

(14) Olivier-Bourbigou, H.; Magna, L.; Morvan, D. *Applied Catalysis a-General* **2010**, *373*, 1-56.

(15) Armand, M.; Endres, F.; MacFarlane, D. R.; Ohno, H.; Scrosati, B. *Nat. Mater.* **2009**, *8*, 621-629.

(16) Chambreau, S. D.; Schneider, S.; Rosander, M.; Hawkins, T.; Gallegos, C. J.; Pastewait, M. F.; Vaghjiani, G. L. *J. Phys. Chem. A* **2008**, *112*, 7816-7824.

(17) Joo, Y. H.; Gao, H. X.; Zhang, Y. Q.; Shreeve, J. M. *Inorg. Chem.* **2010**, *49*, 3282-3288.

(18) Schneider, S.; Hawkins, T.; Rosander, M.; Vaghjiani, G.; Chambreau, S.; Drake, G. *Energy Fuels* **2008**, *22*, 2871-2872.

(19) He, L.; Tao, G. H.; Parrish, D. A.; Shreeve, J. M. *Chemistry-a European Journal* **2009**, *16*, 5736-5743.

(20) Plechkova, N. V.; Seddon, K. R. *Chem. Soc. Rev.* **2008**, *37*, 123-150.

(21) Lovelock, K. R. J.; Deyko, A.; Corfield, J. A.; Gooden, P. N.; Licence, P.; Jones, R. G. *ChemPhysChem* **2009**, *10*, 337-340.

(22) Vitorino, J.; Leal, J. P.; Licence, P.; Lovelock, K. R. J.; Gooden, P. N.; da Piedade, M. E. M.; Shimizu, K.; Rebelo, L. P. N.; Lopes, J. N. C. *ChemPhysChem* **2010**, *11*, 3673-3677.

(23) Wang, C. M.; Luo, H. M.; Li, H. R.; Dai, S. *Phys. Chem. Chem. Phys.* **2010**, *12*, 7246-7250.

(24) Armstrong, J. P.; Hurst, C.; Jones, R. G.; Licence, P.; Lovelock, K. R. J.; Satterley, C. J.; Villar-Garcia, I. J. *Phys. Chem. Chem. Phys.* **2007**, *9*, 982-990.

(25) Gross, J. H. *J. Am. Soc. Mass Spectrom.* **2008**, *19*, 1347-1352.

(26) Chambreau, S. D.; Vaghjiani, G. L.; To, A.; Koh, C.; Strasser, D.; Kostko, O.; Leone, S. R. *J. Phys. Chem. B* **2010**, *114*, 1361-1367.

(27) Akai, N.; Parazs, D.; Kawai, A.; Shibuya, K. *J. Phys. Chem. B* **2009**, *113*, 4756-4762.

(28) Strasser, D.; Goulay, F.; Kelkar, M. S.; Maginn, E. J.; Leone, S. R. *J. Phys. Chem. A* **2007**, *111*, 3191-3195.

(29) Strasser, D.; Goulay, F.; Belau, L.; Kostko, O.; Koh, C.; Chambreau, S. D.; Vaghjiani, G. L.; Ahmed, M.; Leone, S. R. *J. Phys. Chem. A* **2010**, *114*, 879-883.

(30) Leal, J. P.; Esperanca, J.; da Piedade, M. E. M.; Lopes, J. N. C.; Rebelo, L. P. N.; Seddon, K. R. *J. Phys. Chem. A* **2007**, *111*, 6176-6182.

(31) Esperanca, J.; Lopes, J. N. C.; Tariq, M.; Santos, L.; Magee, J. W.; Rebelo, L. P. N. *J. Chem. Eng. Data* **2010**, *55*, 3-12.

(32) Ludwig, R.; Kragl, U. *Angewandte Chemie-International Edition* **2007**, *46*, 6582-6584.

(33) Kelkar, M. S.; Maginn, E. J. *J. Phys. Chem. B* **2007**, *111*, 9424-9427.

(34) Earle, M. J.; Esperanca, J.; Gilea, M. A.; Lopes, J. N. C.; Rebelo, L. P. N.; Magee, J. W.; Seddon, K. R.; Widegren, J. A. *Nature* **2006**, *439*, 831-834.

(35) Vekey, K. *J. Mass Spectrom.* **1996**, *31*, 445-463.

(36) Farmer, D. K.; Matsunaga, A.; Docherty, K. S.; Surratt, J. D.; Seinfeld, J. H.; Ziemann, P. J.; Jimenez, J. L. *Proc. Natl. Acad. Sci. U. S. A.* **2010**, *107*, 6670-6675.

(37) Kroll, J. H.; Smith, J. D.; Che, D. L.; Kessler, S. H.; Worsnop, D. R.; Wilson, K. R. *Phys. Chem. Chem. Phys.* **2009**, *11*, 8005-8014.

(38) Wilson, K. R.; Jimenez-Cruz, M.; Nicolas, C.; Belau, L.; Leonet, S. R.; Ahmed, M. *J. Phys. Chem. A* **2006**, *110*, 2106-2113.

(39) Nash, D. G.; Liu, X. F.; Mysak, E. R.; Baer, T. *Int. J. Mass Spectrom.* **2005**, *241*, 89-97.

(40) Baer, T.; Johnston, M. V.; Nash, D. G. *Int. J. Mass Spectrom.* **2006**, *258*, 2-12.

(41) DeCarlo, P. F.; Kimmel, J. R.; Trimborn, A.; Northway, M. J.; Jayne, J. T.; Aiken, A. C.; Gonin, M.; Fuhrer, K.; Horvath, T.; Docherty, K. S.; Worsnop, D. R.; Jimenez, J. L. *Anal. Chem.* **2006**, *78*, 8281-8289.

(42) Fredlake, C. P.; Crosthwaite, J. M.; Hert, D. G.; Aki, S.; Brennecke, J. F. *J. Chem. Eng. Data* **2004**, *49*, 954-964.

(43) Belau, L.; Wilson, K. R.; Leone, S. R.; Ahmed, M. *J. Phys. Chem. A* **2007**, *111*, 7562-7568.

(44) Leone, S. R.; Ahmed, M.; Wilson, K. R. *Phys. Chem. Chem. Phys.* **2010**, *12*, 6564-6578.

(45) Smith, J. D.; Kroll, J. H.; Cappa, C. D.; Che, D. L.; Liu, C. L.; Ahmed, M.; Leone, S. R.; Worsnop, D. R.; Wilson, K. R. *Atmos. Chem. Phys.* **2009**, *9*, 3209-3222.

Figure Captions

Figure 1. Schematic molecular structure drawings of ionic liquids, (a) 1-Ethyl-3-Methyl-Imidazolium ([$Emim^+$]) Bis(trifluoromethylsulfonyl)imide ([Tf_2N^-]), [$Emim^+$][Tf_2N^-], and (b) 1-Butyl-3-Methyl-Imidazolium ([$Bmim^+$]) Dicyanamide ([Dca^-]), [$Bmim^+$][Dca^-].

Figure 2. Aerosol particle size distribution of ionic liquid, (a) [$Emim^+$][Tf_2N^-] and (b) [$Bmim^+$][Dca^-] with median diameter of 184 ± 3 nm and 187 ± 3 nm respectively, obtained by atomizing 0.5 g/L aqueous solutions.

Figure 3. Mass spectra of (a) [$Emim^+$][Tf_2N^-] from effusive beam (top) and aerosol source beam (bottom) at a photon energy of 9.5 eV with intact cation ($Emim^+$, 111 amu/q) highlighted in grey. Each mass spectrum of the effusive beam (top) and the aerosol source beam (bottom) is collected with mass resolution of 480 and 1061 at 96 amu/q, respectively. (b) Photoionization efficiency (PIE) curves of the intact cation ($Emim^+$) from [$Emim^+$][Tf_2N^-] aerosol particles of total signal (○), which is the raw data collected upon aerosol vaporization, residual signal (●) that is measured without immediately vaporizing the aerosol particles, and the subtracted signal that is the pure contribution of immediately vaporized aerosol particles (total−residue, ▲) at 473 K. (c) Comparison of the photoionization efficiency curves of the intact cation ($Emim^+$) from two different sources, Effusive beam (○), and Aerosol source beam (▲) with the area of error in grey.

Figure 4. Photoionization mass spectra of hypergolic ionic liquid, [$Bmim^+$][Dca^-], at photon energy of (a) 8.5 and (b) 9.4 eV obtained from effusive beam and aerosol source beam both vaporized at 473 K. Intact cation, $Bmim^+$ (139 amu), that represents the ion pair is detected at both photon energies, whereas fragments of 178 amu (([$Bmim^+$]–H)+NCN) and 124 amu

(([$Bmim^+$]–CH_3) or [$Bim]^+$) dominate in the mass spectrum of the effusive beam with little indication of the ion pair at 139 amu. Mass spectra of the aerosol source beam has better signal-to-noise of ca. 800 with 2,000,000 pulses of integration than the effusive beam which has signal-to-noise of ca. 7 with 500,000 pulses of integration.

Figure 5. Molecule (M) to Fragment (F) ratio for ion pairs of [$Bmim^+$][Dca^-] from aerosol source beam (M/F Ratio, 139 amu/137 amu) (a) as a function of temperature at photon energy of 8.5 eV and (b) as a function of photon energy at vaporization temperature of 473 K.

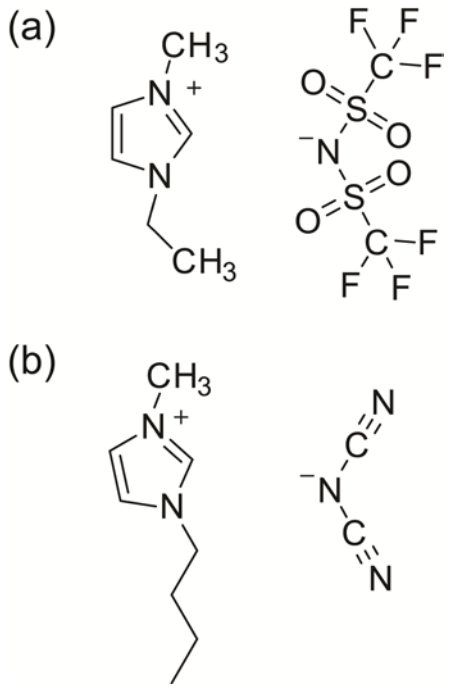

Figure 1. Schematic molecular structure drawings of ionic liquids, (a) 1-Ethyl-3-Methyl-Imidazolium ([Emim$^+$]) Bis(trifluoromethylsulfonyl)imide ([Tf_2N^-]), [Emim$^+$][Tf_2N^-], and (b) 1-Butyl-3-Methyl-Imidazolium ([Bmim$^+$]) Dicyanamide ([Dca^-]), [Bmim$^+$][Dca^-].

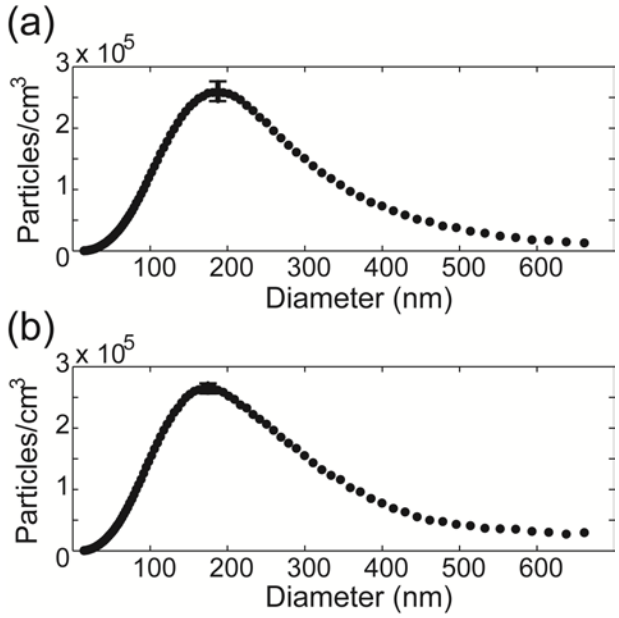

Figure 2. Aerosol particle size distribution of ionic liquid, (a) [$Emim^+$][Tf_2N^-] and (b) [$Bmim^+$][Dca^-] with median diameter of 184 ± 3 nm and 187 ± 3 nm respectively, obtained by atomizing 0.5 g/L aqueous solutions.

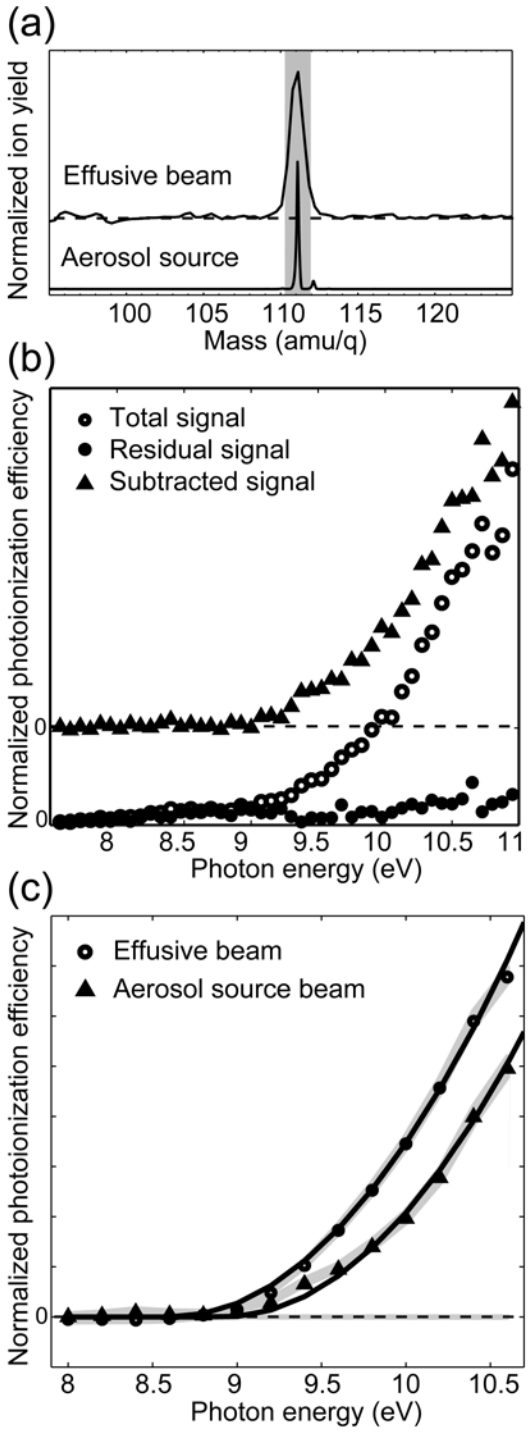

Figure 3. Mass spectra of (a) [$Emim^+$][Tf_2N^-] from effusive beam (top) and aerosol source beam (bottom) at a photon energy of 9.5 eV with intact cation ($Emim^+$, 111 amu/q) highlighted in grey. Each mass spectrum of the effusive beam (top) and the aerosol source beam (bottom) is collected with mass resolution of 480 and 1061 at 96 amu/q, respectively. (b) Photoionization efficiency

(PIE) curves of the intact cation ($Emim^+$) from [$Emim^+$][Tf_2N^-] aerosol particles of total signal (○), which is the raw data collected upon aerosol vaporization, residual signal (●) that is measured without immediately vaporizing the aerosol particles, and the subtracted signal that is the pure contribution of immediately vaporized aerosol particles (total−residue, ▲) at 473 K. (c) Comparison of the photoionization efficiency curves of the intact cation ($Emim^+$) from two different sources, Effusive beam (○), and Aerosol source beam (▲) with the area of error in grey.

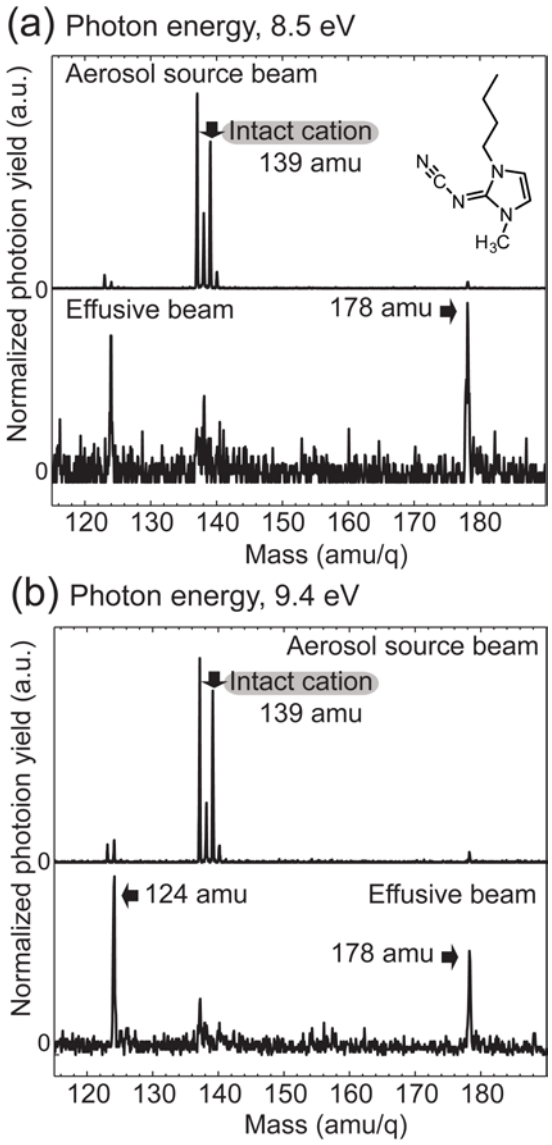

Figure 4. Photoionization mass spectra of hypergolic ionic liquid, [Bmim$^+$][Dca$^-$], at photon energy of (a) 8.5 and (b) 9.4 eV obtained from effusive beam and aerosol source beam both vaporized at 473 K. Intact cation, Bmim$^+$ (139 amu), that represents the ion pair is detected at both photon energies, whereas fragments of 178 amu (([Bmim$^+$]–H)+NCN) and 124 amu (([Bmim$^+$]–CH_3) or [Bim]$^+$) dominate in the mass spectrum of the effusive beam with little indication of the ion pair at 139 amu. Mass spectra of the aerosol source beam has better signal-to-noise of ca. 800 with 2,000,000 pulses of integration than the effusive beam which has signal-to-noise of ca. 7 with 500,000 pulses of integration.

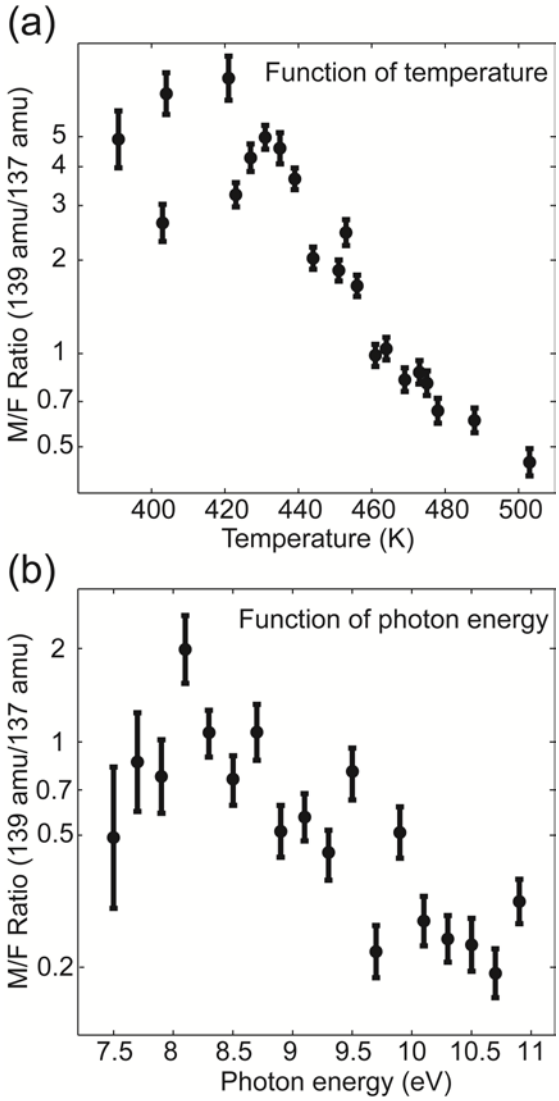

Figure 5. Molecule (M) to Fragment (F) ratio for ion pairs of [$Bmim^+$][Dca^-] from aerosol source beam (M/F Ratio, 139 amu/137 amu) (a) as a function of temperature at photon energy of 8.5 eV and (b) as a function of photon energy at vaporization temperature of 473 K.

Table Of Content (TOC) image